ACCOUNTS
of chemical research

A Natural Vanishing Act: The Enzyme-Catalyzed Degradation of Carbon Nanomaterials

GREGG P. KOTCHEY,[†] SAAD A. HASAN,[†]
ALEXANDER A. KAPRALOV,[‡] SEUNG HAN HA,[§] KANG KIM,[§]
ANNA A. SHVEDOVA,[⊥,∥] VALERIAN E. KAGAN,[‡] AND
ALEXANDER STAR*,[†]

[†]*Department of Chemistry,* [‡]*Department of Environmental and Occupational Health, and* [§]*Department of Medicine, University of Pittsburgh, Pittsburgh, Pennsylvania, United States,* [⊥]*Pathology and Physiology Research Branch, Health Effects Laboratory Division, National Institute for Occupational Safety and Health (NIOSH/CDC), Morgantown, West Virginia, United States, and* [∥]*Department of Physiology and Pharmacology, School of Medicine, West Virginia University, Morgantown, West Virginia, United States*

RECEIVED ON APRIL 11, 2012

CONSPECTUS

Over the past three decades, revolutionary research in nanotechnology by the scientific, medical, and engineering communities has yielded a treasure trove of discoveries with diverse applications that promise to benefit humanity. With their unique electronic and mechanical properties, carbon nanomaterials (CNMs) represent a prime example of the promise of nanotechnology with applications in areas that include electronics, fuel cells, composites, and nanomedicine. Because of toxicological issues associated with CNMs, however, their full commercial potential may not be achieved. The *ex vitro*, *in vitro*, and *in vivo* data presented in this Account provide fundamental insights into the biopersistence of CNMs, such as carbon nanotubes and graphene, and their oxidation/biodegradation processes as catalyzed by peroxidase enzymes. We also communicate our current understanding of the mechanism for the enzymatic oxidation and biodegradation. Finally, we outline potential future directions that could enhance our mechanistic understanding of the CNM oxidation and biodegradation and could yield benefits in terms of human health and environmental safety.

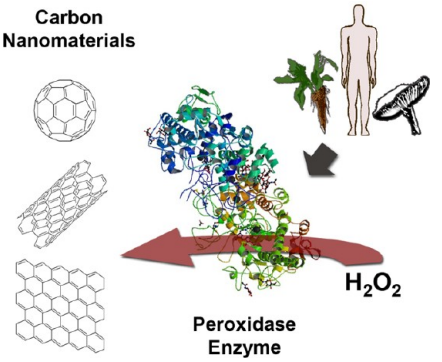

The conclusions presented in this Account may catalyze a rational rethinking of CNM incorporation in diverse applications. For example, armed with an understanding of how and why CNMs undergo enzyme-catalyzed oxidation and biodegradation, researchers can tailor the structure of CNMs to either promote or inhibit these processes. In nanomedical applications such as drug delivery, the incorporation of carboxylate functional groups could facilitate biodegradation of the nanomaterial after delivery of the cargo. On the other hand, in the construction of aircraft, a CNM composite should be stable to oxidizing conditions in the environment. Therefore, pristine, inert CNMs would be ideal for this application. Finally, the incorporation of CNMs with defect sites in consumer goods could provide a facile mechanism that promotes the degradation of these materials once these products reach landfills.

Introduction

Carbon nanotubes and graphene, the nanoscale sp^2 allotropes of carbon, have garnered widespread attention as a result of their remarkable electrical, mechanical, and optical properties and the promise of new technologies that harness these properties. Today, these breakthroughs no longer remain just a vision. The Project on Emerging Nanotechnologies has documented over 30 products containing these carbon nanomaterials (CNMs), in the form of composites, dispersions, and solid-state devices, from a broad selection of industries: aerospace, consumer electronics, cosmetics, and sporting goods.[1] The manufacture and eventual disposal of these products may result in the release of CNMs into the environment and subsequent exposure of humans, animals, and vegetation to these CNMs. Given possible pro-inflammatory and toxic effects of CNMs, much attention has been

Published on the Web 07/23/2012 www.pubs.acs.org/accounts
10.1021/ar300106h

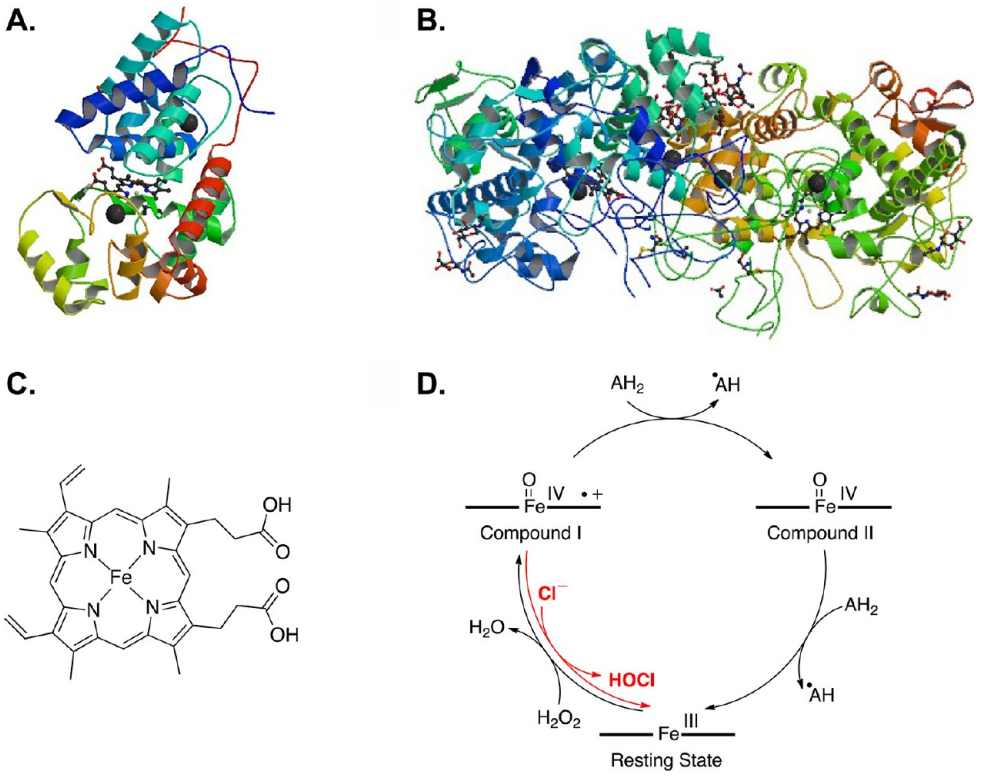

FIGURE 1. Three-dimensional rendering of X-ray crystal structures for (A) horseradish peroxidase (HRP) isoenzyme C and (B) myeloperoxidase (MPO) derived from human leukocytes. (C) Structure of the enzymes' active site, an Fe(III) protoporphyrin IX heme group. (D) The catalytic peroxidase cycle for HRP and MPO. For MPO, compound I is reduced directly to the resting state via conversion of Cl^- to hypochlorous acid in the neutrophils (red path). Panels A and B obtained from the Protein Data Bank, accession codes 1H5A and 3F9P, respectively. Panel D adapted from ref 19. Copyright Elsevier 2004.

SCHEME 1. Chemical Methods To Oxidize Carbon Nanomaterials (CNMs)

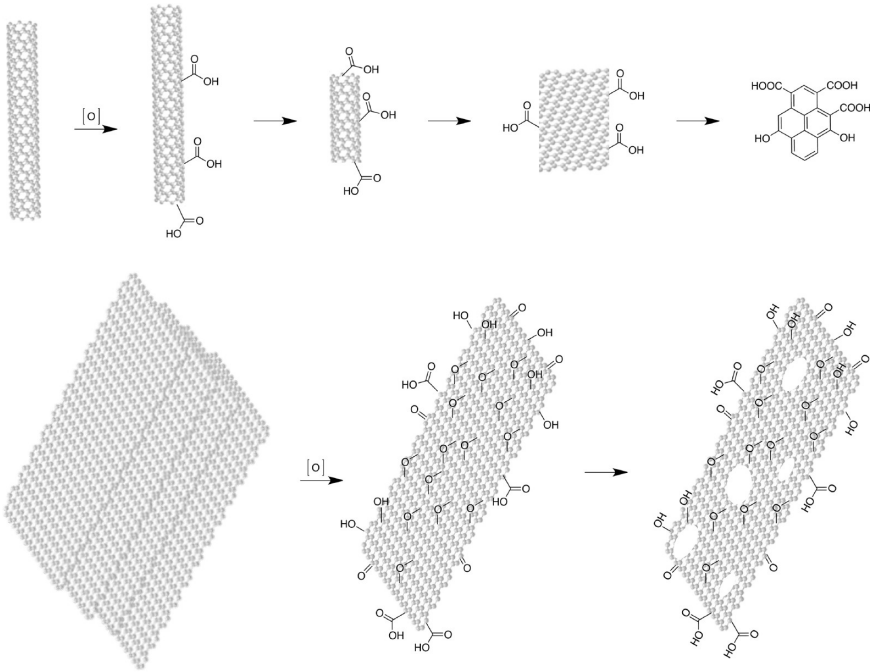

[O] = HNO_3 I H_2SO_4/HNO_3 I $KMnO_4/H_2SO_4$ I NaOCl I H_2O_2/H_2SO_4 I O_3 ($O_2/h\nu$)

focused on their health effects and interactions with living systems,[2−6] with other review articles addressing the distribution, toxicity, and persistence of CNMs in the environment.[7−9]

Recently, several groups have reported the degradation of CNMs catalyzed by naturally occurring enzymes from plants and humans. These findings suggest that the potentially detrimental effects of CNMs associated with their biopersistence may be mitigated thereby enabling these materials to be used more widely in a safe manner. In this Account, we review these findings and discuss possible mechanisms of enzymatic degradation. We relate the oxidative potencies of these enzymes to those of inorganic oxidants employed to oxidize/degrade CNMs. We further elucidate the role of chemical functionalization in CNM degradation. Finally, we discuss data relating to the oxidative biodegradation of CNMs both *in vitro*[10] and *in vivo*[11] as potential means to mitigate the distribution and toxicological effects of CNMs after exposure.

Chemical Oxidation of Carbon Nanomaterials

The scientific literature is rich with reports regarding the covalent modification of CNMs[12−15] with those relating to oxidizing processes summarized in Scheme 1. Strong oxidants, such as H_2SO_4 and HNO_3, disrupt the sp^2 carbon lattice of unfunctionalized CNMs and introduce oxygen-containing functional groups. Typical morphological changes accompanying such oxidation are a decrease in length for nanotubes[16] and the appearance of holes in graphene sheets.[17] Sustained oxidation leads to a loss of material from the carbon framework in the form of byproduct such as CO, CO_2, and aliphatic and polyaromatic hydrocarbons.[10,18] While it was clearly demonstrated in the literature that strong oxidants can oxidize CNMs, these nanomaterials were largely considered to be biopersistent under physiological conditions and in the environment. We, however, hypothesized that like biodegradable polymers CNMs may undergo enzymatic oxidative modifications and biodegradation both *in vivo* and in the environment.

Introduction to Peroxidase Enzymes Utilized for CNM Degradation or Biodegradation

To date, primarily two peroxidase enzymes, horseradish peroxidase (HRP, Figure 1A) and myeloperoxidase (MPO, Figure 1B) have been studied for the degradation or biodegradation of CNMs. For over a century, HRP (molecular weight ∼44 kDa), an enzyme secreted by the root of the horseradish plant (*Armoracia rusticana*), has been utilized in chemical synthesis, biotechnology, and bioremediation.[19]

TABLE 1. Redox Potentials of Peroxidases Used To Oxidize Carbon Nanomaterials

enzyme	step on the peroxidase cycle	E^0 (V)
HRP[24]	compound I/compound II	0.941
	compound II/resting state	0.960
MPO[22]	compound I/resting state	1.16
	compound I/compound II	1.35
	compound II/resting state	0.97

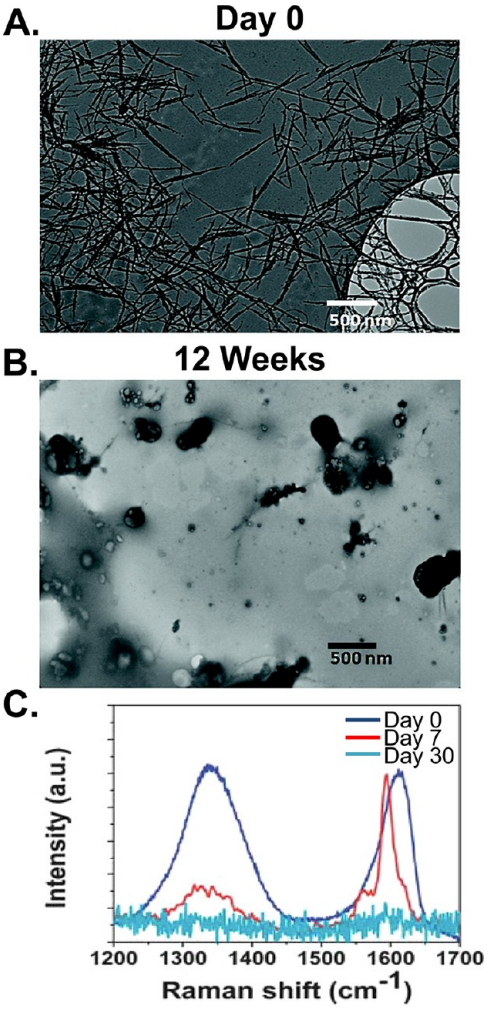

FIGURE 2. TEM images of carboxylated single-walled carbon nanotubes (SWCNTs) incubated with horseradish peroxidase (HRP) and H_2O_2 at 4 °C (A) initially and (B) after 12 weeks. (C) Raman spectra depicting the change in graphitic structure of SWCNTs as a result of HRP/H_2O_2 catalyzed degradation at days 0 (blue), 7 (red), and 30 (cyan). Panels A and B adapted from ref 25. Copyright 2008 American Chemical Society. Panel C adapted from ref 27. Copyright 2011 Royal Society of Chemistry.

Another enzyme, MPO, consisting of two identical dimers with a total weight ∼144 kDa, is expressed in inflammatory cells (predominantly neutrophils) of animals and humans. MPO generates reactive intermediates and oxidants that serve to destroy infecting bacteria.[20−22]

SCHEME 2. The Longitudinal Unzipping of Single-Walled Carbon Nanotubes (SWCNTs)

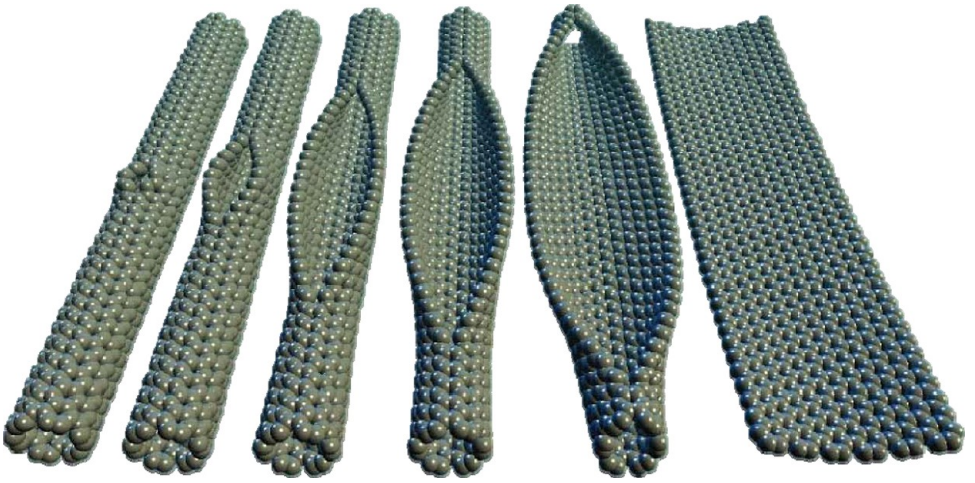

Reproduced from ref 28. Copyright Macmillan Publishers Ltd. 2009.

Both HRP and MPO contain a heme group as their active sites, which is an Fe(III) protoporphyrin IX (Figure 1C). When the enzymes are inactive, the heme group is in the ferric resting state (Figure 1D). In the presence of hydrogen peroxide (H_2O_2), the heme group undergoes a protein-assisted conversion to a ferryl oxo iron (Fe^{4+}=O) porphyrin π cation radical known as compound I, which is subsequently returned to the ferric resting state in two sequential, one-electron transfer steps.[19,22] In the first step, the transient intermediate, compound II, forms when the porphyrin π cation radical is reduced as a substrate (AH_2) is oxidized.[19,22] AH_2 is further oxidized when the ferryl oxo iron is reduced to the ferric resting state.[19,22] Under the acidic conditions of the neutrophil and in the presence of chloride (Cl^-), compound I of MPO abstracts two electrons from Cl^- to yield hypochlorous acid (HOCl) as it returns to the ferric resting state.[22]

Table 1 lists the redox potentials of HRP and MPO. While HRP is a weaker oxidant than MPO, the redox potentials of HRP are comparable to nitric acid (0.957 V).[23] Moreover, HOCl, which has a redox potential of 1.48 V,[23] functions as a stronger oxidant than MPO at each of its steps of the peroxidase cycle.

HRP/H_2O_2-Catalyzed Degradation of CNMs

We demonstrated that carboxylated single-walled carbon nanotubes (SWCNTs) underwent morphological changes (shortening and deformation) when statically incubated at 4 °C in the presence of HRP and H_2O_2 (~40 μM).[25] By transmission electron microscopy (TEM), SWCNTs with a mean length ~500 nm (Figure 2A) were observed to shorten by ~45% over 8 weeks, and mostly residual globular material was detected at 12 weeks (Figure 2B). In contrast, pristine SWCNTs failed to degrade when incubated with HRP and H_2O_2 (~80 μM), from which we theorized that defects or functionalized sites were important facilitators of enzymatic action.[26] Bianco and co-workers corroborated these findings in a study of HRP/H_2O_2 treatment over 30 days, using Raman spectroscopy to monitor changes in the carbon lattice (Figure 2C).[27] The initial Raman spectrum exhibited a strong D band, which was attributed to SWCNT carboxylation. After 7 days of incubation, the D band weakened, suggesting that highly carboxylated nanotubes were oxidized first; on day 30, no Raman signal was observed because the nanotubes were completely oxidized. During the degradation process, the SWCNTs were observed to open via an unzipping mechanism yielding graphene sheets. This result was consistent with recent reports by Tour and co-workers[28] and Dai and co-workers,[29] which revealed that chemical treatments could longitudinally unzip both SWCNTs and MWCNTs to produce graphene nanoribbons (GNRs, Scheme 2).

More recently, the investigation of CNM degradation was expanded to multiwalled carbon nanotubes (MWCNTs). In one study, Bianco and co-workers subjected chemically carboxylated MWCNTs to HRP/H_2O_2 treatment, and over 60 days, MWCNTs were observed to shorten between 25% and 63% (Figure 3A). The observed shortening contrasts the unzipping observed for SWCNTs treated under identical conditions.[27] Independently, during an 80 day study, we investigated the process of MWCNT degradation catalyzed by HRP/H_2O_2.[30] TEM, including high-resolution imaging, revealed that carboxylated MWCNTs decreased in both length

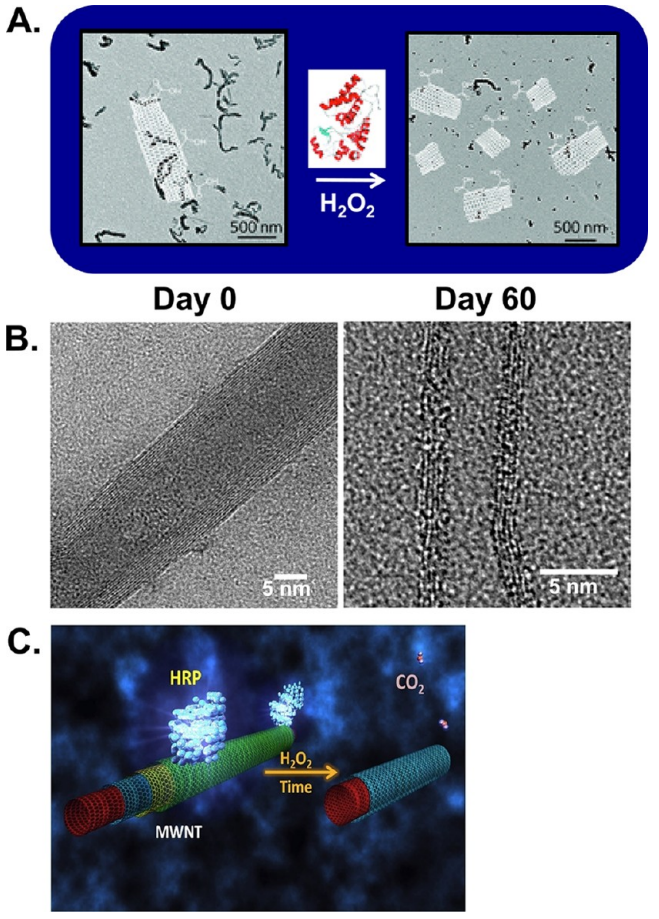

FIGURE 3. (A) Schematic and transmission electron micrographs depicting the shortening of carboxylated multiwalled carbon nanotubes (MWCNTs) catalyzed by horseradish peroxidase (HRP) and H_2O_2. (B) High-resolution TEM images of carboxylated MWCNT before (left) and after (right) 60 days of enzymatic degradation, revealing a thinner nanotube after degradation. (C) Illustration of the mechanism of MWCNT degradation, in which carboxylated MWCNTs were oxidized and exfoliated layer-by-layer to yield pristine inner walls that were more resistant to HRP degradation. Panel A reproduced from ref 27. Copyright 2011 Royal Society of Chemistry. Panels B and C reproduced from ref 30. Copyright 2011 American Chemical Society.

and diameter (Figure 3B), but unlike SWCNTs treated with HRP/H_2O_2, MWCNTs failed to disappear.[30] The decrease in length, in agreement with the report by Bianco and co-workers,[27] suggested that degradation proceeded from the ends of the nanotubes. The concurrent decrease in diameter could be explained by exfoliation of defect-containing outer walls, which were unzipped via the enzymatic oxidation, yielding nanotubes with smaller diameters and possessing mostly pristine outer walls (Figure 3C). The exposure of these newly revealed, more pristine layers coincided with a slowdown in the rate of degradation. Again, we could infer that defects or functionalized sites were important facilitators of enzymatic action. This notion was further supported by our experiments with nitrogen-doped MWCNTs, which were effectively degraded by the HRP/H_2O_2 system over 90 days.[30]

The importance of functionalization for CNM oxidation/degradation by HRP/H_2O_2 was further supported by experiments with graphene oxide (GO), a two-dimensional sheet of oxidized graphitic carbon comprising one layer of carbon atoms decorated with oxygen functionalities like epoxides and carboxylates (Figure 4A). GO incubated with HRP/H_2O_2 was observed via TEM and Raman spectroscopy to undergo enzymatic oxidation.[31] After 8 days of incubation, with daily additions of H_2O_2, holes with a diameter of 2.1 $\pm$ 0.6 nm formed on the basal plane of the GO sheet.[31] By day 10, the diameter of the holes increased more than 12-fold to 26.7 $\pm$ 12.8 nm (Figure 4B), and by day 20, a majority of the GO was oxidized completely. Raman spectroscopy corroborated the TEM observations. In the first 4 days, the D/G intensity ratio increased from 1.1 to 1.6, and on day 20, both the D and G bands disappeared from the signal, indicating progressive oxidation leading to the elimination of the graphitic lattice (Figure 4C). For comparison, the effects of HRP/H_2O_2 treatment on a chemically reduced graphene oxide (RGO) were studied. RGO has the same single-sheet geometry of GO but is mostly devoid of GO's oxygen-containing functional groups. In contrast to GO, the HRP/H_2O_2 treatment failed to oxidize RGO (Figure 4D). Thus, the defect sites introduced by chemical oxidation appeared to have a significant role in the subsequent enzymatic oxidation of the CNM, irrespective of its geometry.

MPO-Catalyzed Degradation of CNMs

Having examined CNM degradation catalyzed by HRP/H_2O_2, we turn to the report of MPO-catalyzed degradation.[10] With the knowledge that human myeloperoxidase (hMPO) degrades implantable polymers such as poly(ester-urea-urethane), we hypothesized that hypochlorite and reactive radical intermediates generated by hMPO would catalyze the oxidation of carboxylated SWCNTs. Nanotube suspensions incubated with the oxidants hMPO/H_2O_2 or hypochlorite appeared lighter in color after 24 h, indicating a decrease in graphitic material (Figure 5A). Moreover, the SWCNT suspension in which NaCl was added to hMPO/H_2O_2 exhibited significant oxidation as evidenced by its nearly clear appearance after 24 h. This result suggested an important role of the strong oxidant, hypochlorous acid, in MPO-catalyzed degradation of CNMs.[32] Raman spectroscopy conducted at intervals up to 24 h showed a progressive decrease in the G band until it was quenched, indicating complete degradation of graphitic lattice (Figure 5B). Vis–NIR absorbance spectroscopy revealed a suppression of

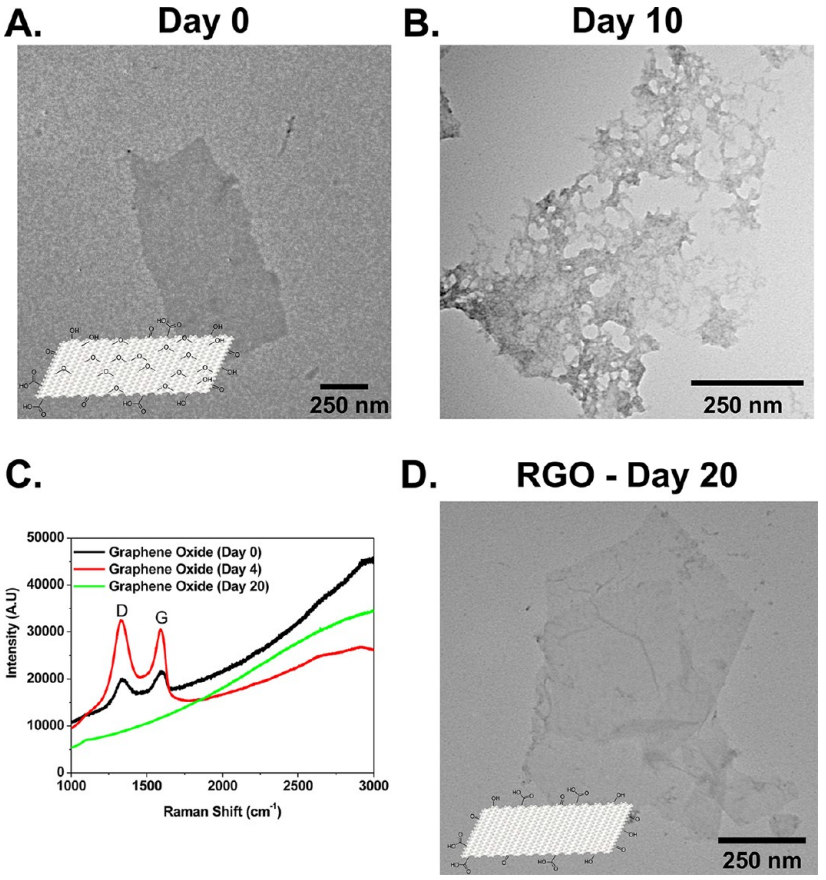

FIGURE 4. TEM micrographs of graphene oxide (GO) (A) initially and (B) after 10 days of incubation with horseradish peroxidase (HRP) and daily additions of 40 μM H_2O_2. (C) Raman spectra of GO and after 0 (black), 4 (red), and 20 (green) days of incubation with HRP/H_2O_2. (D) TEM image of reduced graphene oxide (RGO) after 20 days of identical incubation with HRP/H_2O_2. Reproduced from ref 31. Copyright 2011 American Chemical Society.

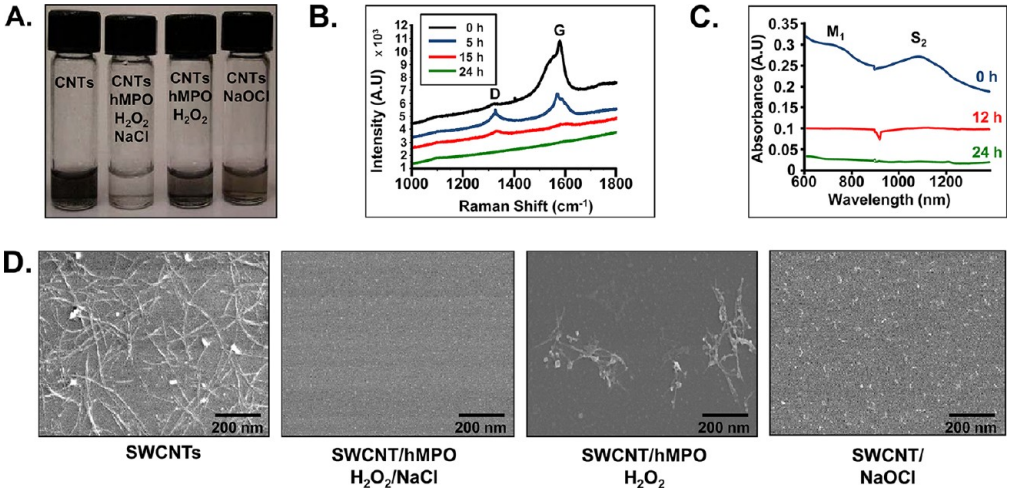

FIGURE 5. (A) Photograph depicting dispersions of carboxylated SWCNTs alone (left) and incubated 24 h under different conditions: hMPO/H_2O_2/NaCl (center-left), hMPO/H_2O_2 (center-right), NaOCl (right). (B) Raman spectra (excitation, 633 nm) of carboxylated SWCNTs (black) and hMPO/H_2O_2-treated carboxylated SWCNTs at 5 (blue), 15 (red), and 24 (green) hours. (C) Vis-NIR spectra depicting the loss of M_1 and S_2 bands during the degradation of carboxylated SWCNTs in hMPO/H_2O_2. (D) Scanning electron micrographs illustrating biodegradation of carboxylated SWNTs (left) after 24 h under different conditions: hMPO/H_2O_2/NaCl (center-left), hMPO/H_2O_2 (center-right), NaOCl (right). Adapted from ref 10. Copyright 2010 Macmillan Publishers Ltd.

TABLE 2. Functionalization of Carbon Nanomaterials and Their Reported *ex Vitro* Degradation by Enzymatic Oxidation

nanomaterial	functionalization	enzyme	oxidant	reported degradation	ref
SWCNT	pristine, unfunctionalized	HRP	H_2O_2	no	26
	carboxylated	HRP	H_2O_2	yes	25−27
	carboxylated	MPO	H_2O_2, NaCl	yes	10,32
	carboxylated/phosphatidylserine	MPO	H_2O_2, NaCl	yes	10
MWCNT	pristine, unfunctionalized	HRP	H_2O_2	no	30
	carboxylated	HRP	H_2O_2	yes	27,30
	1,3-dipolar cycloaddition	HRP	H_2O_2	yes	33
	$CONH(CH_2CH_2O)_2CH_2CH_2NH_3^+$	HRP	H_2O_2	yes	33
	nitrogen-doped	HRP	H_2O_2	yes	30
	$CONH(CH_2CH_2O)_2CH_2CH_2NH_3^+$	MPO	H_2O_2, NaCl	yes	33
graphene	reduced graphene oxide (RGO)	HRP	H_2O_2	no	31
	graphene oxide (GO)	HRP	H_2O_2	yes	31

SCHEME 3. The Effect of Functionalization on CNT Oxidation

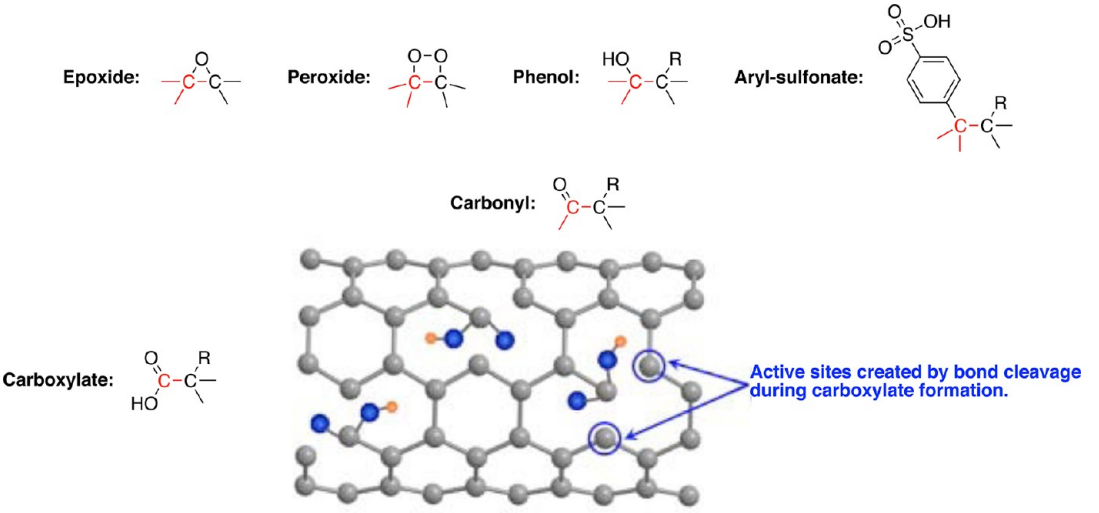

Adapted from ref 34. Copyright Elsevier 2010.

the characteristic semiconducting (S_2) and metallic (M_1) transition bands of SWCNTs in the same interval (Figure 5C). Finally, scanning electron microscopy (SEM) provided direct observation of the morphological changes to the SWCNTs resulting from the different incubation conditions (Figure 5D). For example, after the hMPO/H_2O_2/NaCl treatment, the cylindrical structure that characterizes SWCNTs disappeared (Figure 5D, center left); small quantities of carbonaceous residue remained after incubation with hMPO/H_2O_2 (Figure 5D, center right). Together these measurements showed that hMPO with H_2O_2 catalyzed the degradation of carboxylated SWCNTs, a process further accelerated by the formation of hypochlorite.

The Role of Functional Groups in Enzymatic Oxidation/Degradation

Based on the literature, Table 2 summarizes the reported degradation of CNMs catalyzed by different enzymes. The different functional groups on the CNMs are noted. In a later section, *in vitro* and *in vivo* biodegradation of CNMs will be explored.

A few trends can be gleaned from the *ex vitro* data presented in Table 2. First, minimal enzyme-catalyzed oxidation of pristine (i.e., nonfunctionalized) CNTs and graphene (i.e., RGO) was demonstrated by the available characterization techniques. Alternatively, carboxylated CNTs incubated with either HRP or MPO were further oxidized. Kane and co-workers proposed a mechanism that correlated CNT oxidation to the disruption of the graphitic lattice incurred by functionalization.[34] Strong oxidizing acids employed to functionalize SWCNTs typically yield epoxide, peroxide, hydroxyl, carbonyl, and carboxylate functional groups.[34] During carboxylation, three bonds belonging to the participating carbon atoms are broken, rendering this functionality attached to the graphitic backbone by only one bond (Scheme 3). Thus, carboxylated CNTs appeared most susceptible to enzymatic oxidation, because only one bond

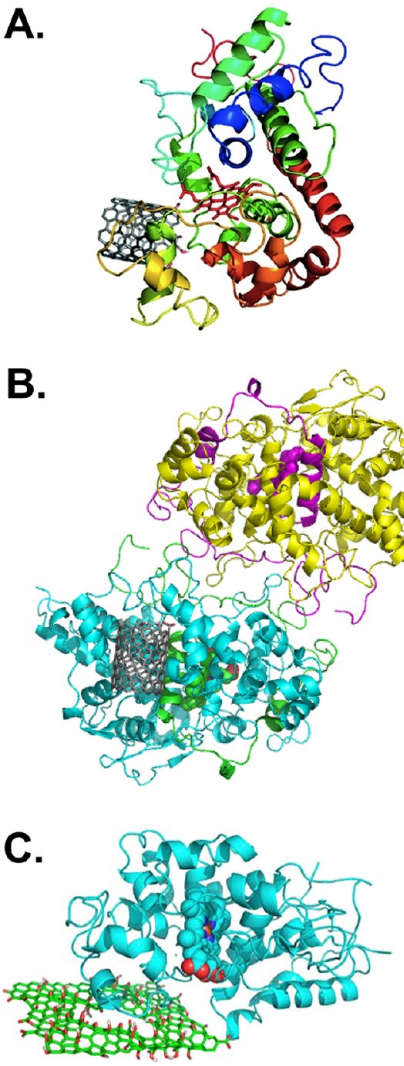

FIGURE 6. Binding poses of (A) horseradish peroxidase (HRP) and (B) myeloperoxidase (MPO) on carboxylated SWCNTs calculated using molecular docking studies (AutoDock Vina). (C) Binding pose of HRP on graphene oxide. Panel A reproduced from ref 26. Copyright 2009 American Chemical Society. Panel B reproduced from ref 10. Copyright Macmillan Publishers Ltd. 2010. Panel C reproduced from ref 31. Copyright 2011 American Chemical Society.

needed to be cleaved. This assertion was further supported by the results shown in Figure 3 for MWCNTs and their proposed oxidation mechanism. After the outer layers containing functional groups (i.e., carboxylates) were enzymatically oxidized and exfoliated, the more pristine inner layers failed to undergo oxidation.

Enzyme–Substrate Interactions in CNM Oxidation/Degradation

We hypothesized that the carboxylates are important for one additional reason: their negative charge in aqueous media facilitates the proper orientation/proximity of the peroxidase

SCHEME 4. Work Function (V) and Standard Potential (E^0) of SWCNTs

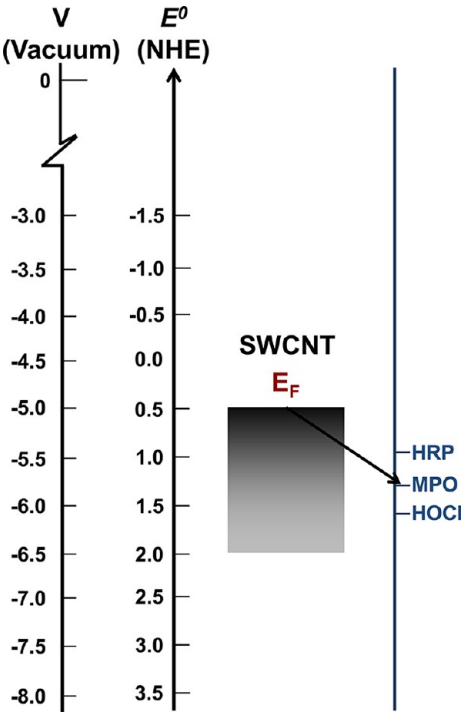

Adapted from ref 35, Copyright Macmillan Publishers Ltd. 2001, and ref 36 Copyright 2002 American Chemical Society.

enzyme's heme active site to the SWCNT substrate. We employed molecular modeling studies to characterize the role of functional groups in enzyme–substrate interactions. A calculation of the docking conformations for carboxylated SWCNTs on HRP predicted that the carboxylated ends, which are negatively charged in an aqueous suspension, would orient themselves toward a positively charged arginine residue, Arg178, near HRP's heme site (Figure 6A).[26] In contrast, pristine SWCNTs, which failed to undergo degradation, were predicted to orient themselves with the distal end of the enzyme away from the active heme site.

Similarly, for MPO, molecular simulations suggested two possible sites for interaction between the enzyme and SWCNTs.[10] The first site, located at the proximal end of the heme group, contained catalytically active tyrosine residues, Tyr293 and Tyr313, and arginine residues, Arg294, Arg307, and Arg507;[10] again, the positively charged arginine residues interact strongly with the negatively charged carboxylated nanotubes (Figure 6B). The second site, at the distal end of the heme group and distant from the tyrosine residues, appeared to bind the pristine SWCNTs.

The molecular modeling of HRP was expanded from the docking of one-dimensional SWCNTs to that of two-dimensional

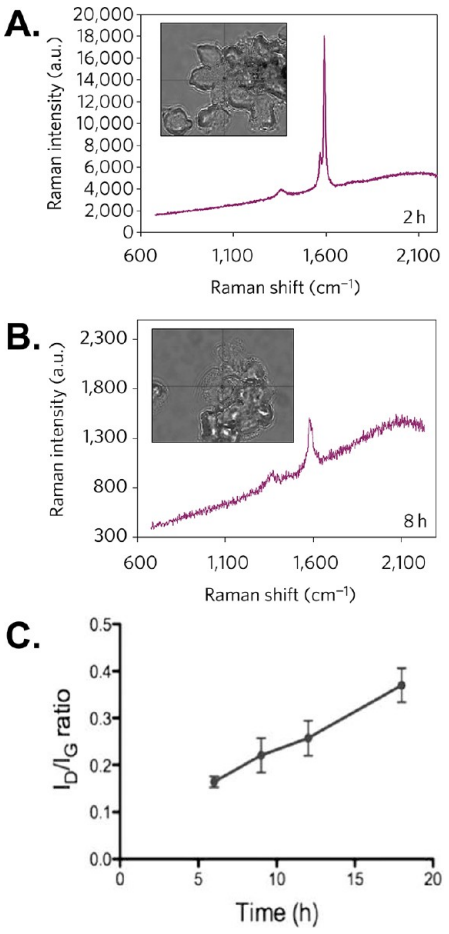

FIGURE 7. Raman spectra (excitation, 473 nm) recorded from different areas of neutrophils containing IgG–nanotubes at (A) 2 h and (B) 8 h. Inset depicts bright-field image of the neutrophils with engulfed IgG–nanotubes with cross-wires depicting location of laser spot. (C) D/G intensity ratios obtained from Raman spectroscopy on double-walled carbon nanotubes (DWCNTs) in PC3 cells at different time points. A trend of increasing defects on the walls of the DWCNTs was observed with the signal-to-noise ratio decreasing at 24 h. Panels A and B reproduced from ref 10. Copyright Macmillan Publishers Ltd. 2010. Panel C reproduced from ref 39. Copyright Wiley-VCH 2010).

graphene sheets.[31] For this geometry, favorable binding poses were identified only on graphene's basal plane (Figure 6C) because the edges of the sheet failed to provide sufficient surface area for graphene–HRP stabilization through hydrophobic interactions. Along the basal plane, the heme active site was situated approximately 8.7 Å from the surface of GO. In contrast, the separation distance for RGO was 11.5 Å. The presence of epoxide and alcohol groups on the basal plane of GO may be responsible for orienting the heme active site with enough proximity to the GO thereby enabling its oxidation catalyzed by HRP/H_2O_2.

Mechanism of the Enzyme-Catalyzed CNM Oxidation and Degradation

Scheme 4 depicts the work function under vacuum (*V*, ~5 eV) and standard potential (E^0, +0.5 V) of the valence band for SWCNTs.[35,36] Since HRP, MPO, and MPO's byproduct, HOCl, are stronger oxidants (i.e., demonstrate more positive redox potentials), these species should be spontaneously reduced under standard conditions by accepting electrons from the valence band of SWCNTs and thereby oxidizing them. While thermodynamically HRP and MPO have the potential to spontaneously oxidize SWCNTs, in reality CNT oxidation and degradation may be influenced by enzyme/substrate interactions and is facilitated by defects.

It has been demonstrated that hypochlorite results in the introduction of acid "defect" sites on the surface of CNTs.[37] Therefore, for MPO-catalyzed biodegradation, it is possible that the initial oxidation of CNMs is predominantly due to the effects of hypochlorite (as a result of its very high oxidizing potential); the accumulation of oxidative "defects" may pave the way for subsequently more effective oxidation via both mechanisms (i.e., hypochlorite and peroxidase reactive intermediates with lower oxidizing potentials).

What is evident from these proposed mechanisms is the need for further investigations to elucidate the enzyme-catalyzed degradation process at the molecular level. By identifying the byproducts of degradation, it will be possible to construct more specific reaction schemes describing the mechanism of the enzyme-catalyzed processes. While this *Account* has focused on the heterolytic bond cleavage of H_2O_2 catalyzed by peroxidase enzymes, an alternative mechanism involving the homolytic cleavage of H_2O_2 catalyzed by transition metals such as iron can also impact CNMs. For example, Smalley and co-workers demonstrated that a metal-catalyzed process could be employed for the purification of SWCNTs,[38] and we established that the radicals generated through the homolytic cleavage of H_2O_2 in the presence of iron and hemin (i.e., via the Fenton reaction) can degrade SWCNTs.[26]

Biological Investigations: *In Vitro* and *in Vivo* Biodegradation of CNMs

While *ex vitro* experiments with HRP and MPO demonstrated the ability of these enzymes to catalyze degradation of CNMs, they did not address the significance of these reactions *in vitro* and *in vivo.* Thus, the enzymatic oxidation of CNMs has been studied in living systems. For carbon nanotubes (CNTs), we employed Raman spectroscopy to monitor

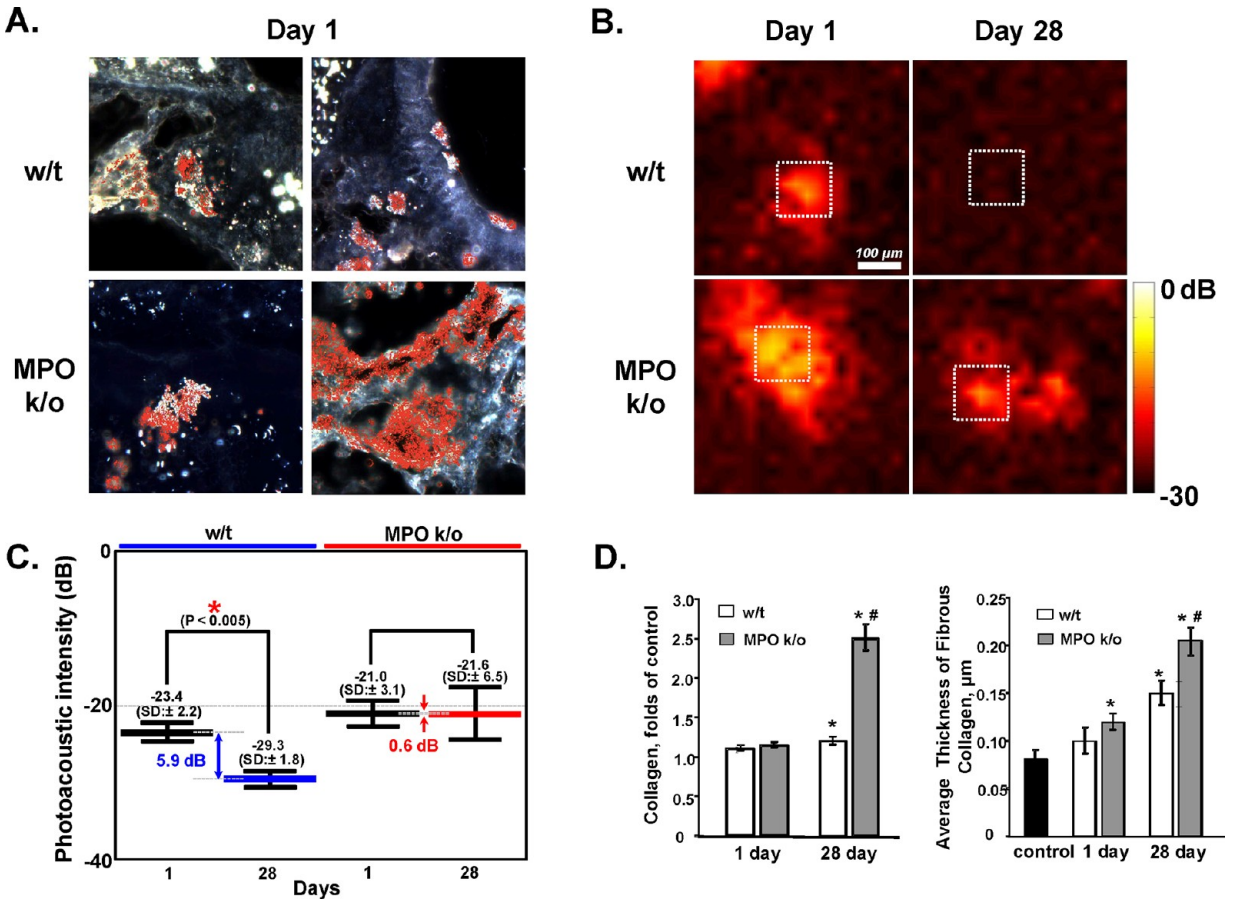

FIGURE 8. (A) Hyperspectral images (CytoViva) of the lung tissue for both w/t and MPO k/o at day 1. The red areas are the pixels that match the SWCNT spectral profiles. The scanned images were collected at 40× employing an Olympus BX-51 microscope and a 100 W quartz-halogen light source. Spectral data was captured with the CytoViva spectrophotometer utilizing an integrated CCD camera. (B) Photoacoustic (PA) images and (C) statistical analysis (student's *t* test) of PA intensity averaged over the region in the box in panel B of a lung section from each group of animals at days 1 and 28. (D) Changes in the content of collagen (left) and the average thickness (right) of alveolar connective tissue in the lungs of w/t and MPO k/o mice at days 1 and 28 after pharyngeal aspiration of SWCNTs. Panel D Reproduced from ref 11.

carboxylated SWCNTs located within neutrophils, inflammatory cells containing high concentrations of MPO. The intensity of the D band relative to the G band increased noticeably going from 2 to 8 h of incubation within the neutrophils (Figure 7A,B). This change suggests the introduction of defects to the nanotubes via enzymatic oxidation. Neves et al. tracked the process further by measuring the Raman signal from oxidized, RNA-wrapped double-walled CNTs incubated with human prostate adenocarcinoma cells for up to 18 h.[39] They reported a steady increase in the D/G intensity ratio with incubation time (Figure 7C) and inferred that this progression was due to defect-inducing alterations in the outer wall of the nanotubes. Unfortunately, they did not pinpoint the actor or mechanism within the cells that altered the structure of the nanotubes' wall. These are interesting experiments in that RNA is also negatively charged; therefore, the positively charged domains in the putative catalyst would act similarly to the peroxidases described above.

Our *in vivo* murine experiments afforded the most important evidence for the role of MPO in oxidative biodegradation of CNTs. In this study, the pulmonary inflammation response of mice exposed to carboxylated SWCNTs via pharyngeal aspiration was compared between wild-type (w/t) mice and MPO-knockout (k/o) mice (i.e., mice with and without MPO, respectively).[11] One of the primary challenges in assessing CNT biodegradation entails quantitatively evaluating the content of the CNM *in vivo*. An interesting opportunity is offered by the Hyperspectral Imaging methodology (CytoViva) whereby spectral signatures characteristic of CNTs are collected into a spectral library and subsequently utilized for the detection of CNT in tissue sections (Figure 8A). Furthermore, photoacoustic (PA) imaging technology[40] was utilized to assess the content of

SWCNTs in sections of the lungs from w/t and MPO k/o mice (Figure 8B). The decreased PA intensity 28 days after pharyngeal aspiration of SWCNTs was statistically significant in w/t mice but not in MPO k/o mice (Figure 8C). Combined with the data obtained by several additional quantitative protocols (Raman microscopy, NIR spectroscopy, TEM analysis), we concluded that the inflammatory response in MPO k/o mice was stronger than that in w/t C57B1/6 mice and that SWCNT oxidation and clearance from the lungs of MPO k/o animals was markedly less effective (Figure 8D).[11] Interestingly, a recent report documented *in vivo* degradation of CNT in the brain of animals.[41]

Outlook and Conclusions

Biopersistence of CNMs has been long viewed as the major factor contributing to the toxic effects of these nanomaterials in the body. The discovery of enzymatic CNT degradation processes,[10,11,25−27,30−32] opened new opportunities for the regulation of CNT distribution and fate *in vivo* by controlling inflammatory response and employing SWCNT-metabolizing enzymes. Indeed, the number of studies relating to the field of CNMs and biodegradation has grown vigorously. For example, PubMed revealed 16 entries using the search terms "biodegrade/biodegradation" and "carbon nanotubes" before 2008; an additional 48 publications have been added since then. Although research in the field has greatly expanded, a significant amount of work is still warranted. To date, most research on enzyme-catalyzed biodegradation has focused on HRP *ex vitro* and MPO *in vitro* and *in vivo*; it is possible that other enzymes such as eosinophil peroxidases (EPO) and lactoperoxidase (LPO) could be involved in the biodegradation process. Furthermore, other hemo-proteins with peroxidase activity merit investigation, including different forms of cytochrome P450, cytochrome *c*, etc. The specific roles and significance of these enzymes in biodegradation and regulation of inflammatory responses should be explored. Additionally, the assessment of the intermediates of biodegradation represents another area of research that merits investigation because the likely products, aliphatic and oxidized polyaromatic hydrocarbons, will provide details about the mechanism of CNM biodegradation and may exert their own specific, possibly toxic, effects on the body, which may also have to be taken into account.

As a result of the revolutionary research on enzyme-catalyzed biodegradation, one can envision futuristic applications in areas like drug delivery or imaging applications. For example, enzymes that result in biodegradation could be encapsulated inside nitrogen-doped nanocapsules,[42] a CNM that could be employed to deliver drug or imaging cargo along with all the components for its self-elimination from the body. More practically, relatively nontoxic and inexpensive enzymes may be instrumental in environmental/occupational biodegradation of CNMs contamination introduced via spills, waste products in landfills, etc. To this end, white-rot basidiomycete fungi that secrete lignin peroxidase (LiP) were exposed to a dispersion of $C_{60}(OH)_n$ and proceeded to oxidize this CNM over 32 weeks.[43] This result suggests the existence of a bioremediation pathway for oxidized CNMs that might otherwise accumulate in the environment. Finally, an interesting avenue of research will be applying enzymatic biodegradation to other noncarbonaceous nanomaterials to mitigate toxicity.

This work was supported by NIEHS R01ES019304, HL70755, HL094488, U19AI068021, NIOSH OH008282 and NORA/NTRC NIOSH 1927ZHF. G.P.K. acknowledges support from the EPA STAR Graduate Fellowship FP-91713801. The findings and conclusions in this report are those of the authors and do not necessarily represent the views of the National Institute for Occupational Safety and Health.

BIOGRAPHICAL INFORMATION

Gregg P. Kotchey received his B.S. degree in chemistry (2004) from the University of Pittsburgh, where he is now working on his Ph.D. under the direction of Professor Alexander Star.

Saad A. Hasan received his Ph.D. in materials science (2010) from Vanderbilt University, after which he joined the Nanommune project at Uppsala University (Sweden). Saad was a postdoctoral associate in Professor Star's group at Pittsburgh.

Alexander A. Kapralov received his Ph.D. in Biochemistry (1986) from Institute of Biochemistry Ukrainian Academy of Sciences (Ukraine) and Dr. Sc. in Biochemistry (2000) from National Kyiv University (Ukraine). He is now a research associate with Professor Kagan at the University of Pittsburgh.

Seung Han Ha received his Ph.D. in Biomedical Engineering (2009) from Korea University; he currently is a postdoctoral associate in Professor Kang Kim's group at Pittsburgh.

Kang Kim is Assistant Professor of Medicine and Bioengineering at the University of Pittsburgh.

Anna A. Shvedova is Lead Research Physiologist at the Pathology and Physiology Research Branch, Health Effects Laboratory Division, National Institute for Occupational Safety and Health (NIOSH/CDC), and adjunct Professor at the Department of Physiology and Pharmacology, School of Medicine, West Virginia University.

Valerian E. Kagan is Professor and Vice Chair in the Department of Environmental and Occupational Health and Director of the

Center for Free Radical and Antioxidant Health at the University of Pittsburgh.

Alexander Star is Associate Professor of Chemistry at Pittsburgh.

FOOTNOTES

*To whom correspondence should be addressed. E-mail: astar@pitt.edu.
The authors declare no competing financial interest.

REFERENCES

1 The project on emerging nanotechnologies. http://www.nanotechproject.org/ (accessed April 9, 2012).

2 Kagan, V. E.; Tyurina, Y. Y.; Tyurin, V. A.; Konduru, N. V.; Potapovich, A. I.; Osipov, A. N.; Kisin, E. R.; Schwegler-Berry, D.; Mercer, R.; Castranova, V.; Shvedova, A. A. Direct and indirect effects of single walled carbon nanotubes on raw 264.7 macrophages: Role of iron. *Toxicol. Lett.* **2006**, *165*, 88–100.

3 Tkach, A. V.; Shurin, G. V.; Shurin, M. R.; Kisin, E. R.; Murray, A. R.; Young, S.-H.; Star, A.; Fadeel, B.; Kagan, V. E.; Shvedova, A. A. Direct effects of carbon nanotubes on dendritic cells induce immune suppression upon pulmonary exposure. *ACS Nano* **2011**, *5*, 5755–5762.

4 Shvedova, A. A.; Kisin, E. R.; Mercer, R.; Murray, A. R.; Johnson, V. J.; Potapovich, A. I.; Tyurina, Y. Y.; Gorelik, O.; Arepalli, S.; Schwegler-Berry, D.; Hubbs, A. F.; Antonini, J.; Evans, D. E.; Ku, B.-K.; Ramsey, D.; Maynard, A.; Kagan, V. E.; Castranova, V.; Baron, P. Unusual inflammatory and fibrogenic pulmonary responses to single-walled carbon nanotubes in mice. *Am. J. Physiol.* **2005**, *289*, L698–L708.

5 Kisin, E. R.; Murray, A. R.; Keane, M. J.; Shi, X.-C.; Schwegler-Berry, D.; Gorelik, O.; Arepalli, S.; Castranova, V.; Wallace, W. E.; Kagan, V. E.; Shvedova, A. A. Single-walled carbon nanotubes: Geno- and cytotoxic effects in lung fibroblast v79 cells. *J. Toxicol. Environ. Health, Part A* **2007**, *70*, 2071–2079.

6 Shvedova, A. A.; Fabisiak, J. P.; Kisin, E. R.; Murray, A. R.; Roberts, J. R.; Tyurina, Y. Y.; Antonini, J. M.; Feng, W. H.; Kommineni, C.; Reynolds, J.; Barchowsky, A.; Castranova, V.; Kagan, V. E. Sequential exposure to carbon nanotubes and bacteria enhances pulmonary inflammation and infectivity. *Am. J. Respir. Cell Mol. Biol.* **2008**, *38*, 579–590.

7 Pérez, S.; Farré, M. L.; Barceló, D. Analysis, behavior and ecotoxicity of carbon-based nanomaterials in the aquatic environment. *TrAC, Trends Anal. Chem.* **2009**, *28*, 820–832.

8 Petersen, E. J.; Zhang, L.; Mattison, N. T.; O'Carroll, D. M.; Whelton, A. J.; Uddin, N.; Nguyen, T.; Huang, Q.; Henry, T. B.; Holbrook, R. D.; Chen, K. L. Potential release pathways, environmental fate, and ecological risks of carbon nanotubes. *Environ. Sci. Technol.* **2011**, *45*, 9837–9856.

9 Eckelman, M. J.; Mauter, M. S.; Isaacs, J.; Elimelech, M. New perpsectives on nanomaterial aquatic ecotoxicity: Production impacts exceed direct exposure impacts for carbon nanotubes. *Environ. Sci. Technol.* **2012**, *46*, 2902–2910.

10 Kagan, V. E.; Konduru, N. V.; Feng, W.; Allen, B. L.; Conroy, J.; Volkov, Y.; Vlasova, I. I.; Belikova, N. A.; Yanamala, N.; Kapralov, A.; Tyurina, Y. Y.; Shi, J.; Kisin, E. R.; Murray, A. R.; Franks, J.; Stolz, D.; Gou, P.; Klein-Seetharaman, J.; Fadeel, B.; Star, A.; Shvedova, A. A. Carbon nanotubes degraded by neutrophil myeloperoxidase induce less pulmonary inflammation. *Nat. Nanotechnol.* **2010**, *5*, 354–359.

11 Shvedova, A. A.; Kapralov, A. A.; Feng, W. H.; Kisin, E. R.; Murray, A. R.; Mercer, R. R., St.; Croix, C. M.; Lang, M. A.; Watkins, S. C.; Konduru, N. V.; Allen, B. L.; Conroy, J.; Kotchey, G. P.; Mohamed, B. M.; Meade, A. D.; Volkov, Y.; Star, A.; Fadeel, B.; Kagan, V. E. Impaired clearance and enhanced pulmonary inflammatory/fibrotic response to carbon nanotubes in myeloperoxidase-deficient mice. *PLoS One* **2012**, *7*, No. e30923.

12 Peng, X.; Wong, S. S. Functional covalent chemistry of carbon nanotube surfaces. *Adv. Mater.* **2009**, *21*, 625–642.

13 Karousis, N.; Tagmatarchis, N.; Tasis, D. Current progress on the chemical modification of carbon nanotubes. *Chem. Rev.* **2010**, *110*, 5366–5397.

14 Loh, K. P.; Bao, Q.; Ang, P. K.; Yang, J. The chemistry of graphene. *J. Mater. Chem.* **2010**, *20*, 2277–2289.

15 Dreyer, D. R.; Park, S.; Bielawski, C. W.; Ruoff, R. S. The chemistry of graphene oxide. *Chem. Soc. Rev.* **2010**, *39*, 228–240.

16 Liu, J.; Rinzler, A. G.; Dai, H. J.; Hafner, J. H.; Bradley, R. K.; Boul, P. J.; Lu, A.; Iverson, T.; Shelimov, K.; Huffman, C. B.; Rodriguez-Macias, F.; Shon, Y. S.; Lee, T. R.; Colbert, D. T.; Smalley, R. E. Fullerene pipes. *Science* **1998**, *280*, 1253–1256.

17 Zhao, X.; Hayner, C. M.; Kung, M. C.; Kung, H. H. Flexible holey graphene paper electrodes with enhanced rate capability for energy storage applications. *ACS Nano* **2011**, *5*, 8739–8749.

18 Wang, Z.; Shirley, M. D.; Meikle, S. T.; Whitby, R. L. D.; Mikhalovsky, S. V. The surface acidity of acid oxidised multi-walled carbon nanotubes and the influence of in-situ generated fulvic acids on their stability in aqueous dispersions. *Carbon* **2009**, *47*, 73–79.

19 Veitch, N. C. Horseradish peroxidase: A modern view of a classic enzyme. *Phytochemistry* **2004**, *65*, 249–259.

20 Nauseef, W. M. How human neutrophils kill and degrade microbes: An integrated view. *Immunol. Rev.* **2007**, *219*, 88–102.

21 Hansson, M.; Olsson, I.; Nauseef, W. M. Biosynthesis, processing, and sorting of human myeloperoxidase. *Arch. Biochem. Biophys.* **2006**, *445*, 214–224.

22 Arnhold, J. Properties, functions, and secretion of human myeloperoxidase. *Biochemistry (Moscow)* **2004**, *69*, 4–9.

23 *Potentials*; Lide, D. R., Ed.; CRC Press: Boca Raton, FL, 2004; pp 20−29.

24 Hayashi, Y.; Yamazaki, I. The oxidation-reduction potentials of compound i/compound ii and compound ii/ferric couples of horseradish peroxidases a2 and c. *J. Biol. Chem.* **1979**, *254*, 9101–9106.

25 Allen, B. L.; Kichambare, P. D.; Gou, P.; Vlasova, Ii; Kapralov, A. A.; Konduru, N.; Kagan, V. E.; Star, A. Biodegradation of single-walled carbon nanotubes through enzymatic catalysis. *Nano Lett.* **2008**, *8*, 3899–3903.

26 Allen, B. L.; Kotchey, G. P.; Chen, Y.; Yanamala, N. V. K.; Klein-Seetharaman, J.; Kagan, V. E.; Star, A. Mechanistic investigations of horseradish peroxidase-catalyzed degradation of single-walled carbon nanotubes. *J. Am. Chem. Soc.* **2009**, *131*, 17194–17205.

27 Russier, J.; Menard-Moyon, C.; Venturelli, E.; Gravel, E.; Marcolongo, G.; Meneghetti, M.; Doris, E.; Bianco, A. Oxidative biodegradation of single- and multi-walled carbon nanotubes. *Nanoscale* **2011**, *3*, 893–896.

28 Kosynkin, D. V.; Higginbotham, A. L.; Sinitskii, A.; Lomeda, J. R.; Dimiev, A.; Price, B. K.; Tour, J. M. Longitudinal unzipping of carbon nanotubes to form graphene nanoribbons. *Nature* **2009**, *458*, 872–876.

29 Jiao, L.; Zhang, L.; Wang, X.; Diankov, G.; Dai, H. Narrow graphene nanoribbons from carbon nanotubes. *Nature* **2009**, *458*, 877–880.

30 Zhao, Y.; Allen, B. L.; Star, A. Enzymatic degradation of multiwalled carbon nanotubes. *J. Phys. Chem. A* **2011**, *115*, 9536–9544.

31 Kotchey, G. P.; Allen, B. L.; Vedala, H.; Yanamala, N.; Kapralov, A. A.; Tyurina, Y. Y.; Klein-Seetharaman, J.; Kagan, V. E.; Star, A. The enzymatic oxidation of graphene oxide. *ACS Nano* **2011**, *5*, 2098–2108.

32 Vlasova, I.; Sokolov, A.; Chekanov, A.; Kostevich, V.; Vasilyev, V. Myeloperoxidase-induced biodegradation of single-walled carbon nanotubes is mediated by hypochlorite. *Russ. J. Bioorg. Chem.* **2011**, *37*, 453–463.

33 Bianco, A.; Kostarelos, K.; Prato, M. Making carbon nanotubes biocompatible and biodegradable. *Chem. Commun.* **2011**, *47*, 10182–10188.

34 Liu, X.; Hurt, R. H.; Kane, A. B. Biodurability of single-walled carbon nanotubes depends on surface functionalization. *Carbon* **2010**, *48*, 1961–1969.

35 Gratzel, M. Photoelectrochemical cells. *Nature* **2001**, *414*, 338–344.

36 Choi, H. C.; Shim, M.; Bangsaruntip, S.; Dai, H. Spontaneous reduction of metal ions on the sidewalls of carbon nanotubes. *J. Am. Chem. Soc.* **2002**, *124*, 9058–9059.

37 Yang, J.-C.; Yen, C.-H.; Wang, W.-J.; Horng, J.-J.; Tsai, Y.-P. Assessment of adequate sodium hypochlorite concentration for pre-oxidization of multi-walled carbon nanotubes. *J. Chem. Technol. Biotechnol.* **2010**, *85*, 699–707.

38 Wang; Shan, H.; Hauge, R. H.; Pasquali, M.; Smalley, R. E. A highly selective, one-pot purification method for single-walled carbon nanotubes. *J. Phys. Chem. B* **2007**, *111*, 1249–1252.

39 Neves, V.; Heister, E.; Costa, S.; Tîlmaciu, C.; Borowiak-Palen, E.; Giusca, C. E.; Flahaut, E.; Soula, B.; Coley, H. M.; Mcfadden, J.; Silva, S. R. P. Uptake and release of double-walled carbon nanotubes by mammalian cells. *Adv. Funct. Mater.* **2010**, *20*, 3272–3279.

40 Kim, K.; Huang, S.-W.; Ashkenazi, S.; O'Donnell, M.; Agarwal, A.; Kotov, N. A.; Denny, M. F.; Kaplan, M. J. Photoacoustic imaging of early inflammatory response using gold nanorods. *Appl. Phys. Lett.* **2007**, *90*, No. 223901.

41 Nunes, A.; Bussy, C.; Gherardini, L.; Meneghetti, M.; Herrero, M. A.; Bianco, A.; Prato, M.; Pizzorusso, T.; Al-Jamal, K. T.; Kostarelos, K. In vivo degradation of functionalized carbon nanotubes after stereotactic administration in the brain cortex. *Nanomedicine* **2012**, DOI: 10.2217/nnm.12.33.

42 Allen, B. L.; Shade, C. M.; Yingling, A. M.; Petoud, S.; Star, A. Graphitic nanocapsules. *Adv. Mater.* **2009**, *21*, 4692–4695.

43 Schreiner, K. M.; Filley, T. R.; Blanchette, R. A.; Bowen, B. B.; Bolskar, R. D.; Hockaday, W. C.; Masiello, C. A.; Raebiger, J. W. White-rot basidiomycete-mediated decomposition of C_{60} fullerol. *Environ. Sci. Technol.* **2009**, *43*, 3162–3168.